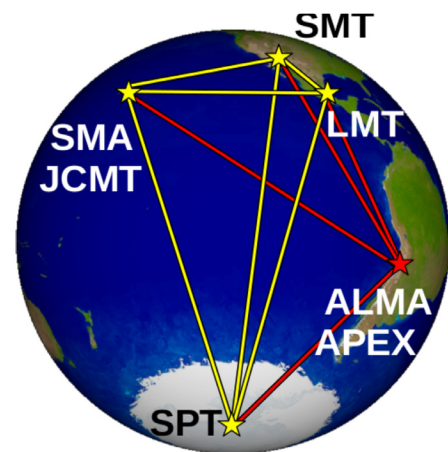
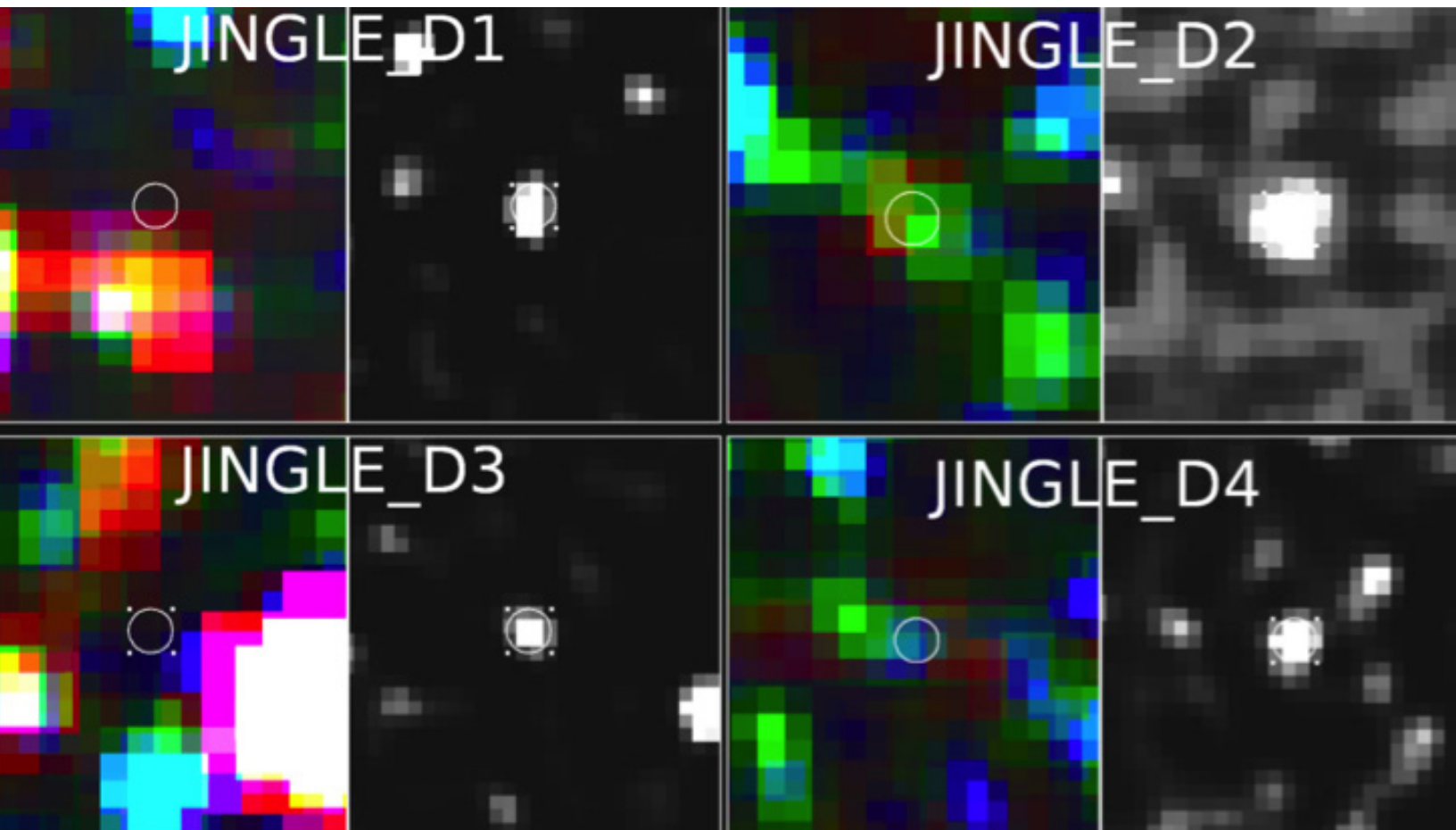


East Asian Observatory News

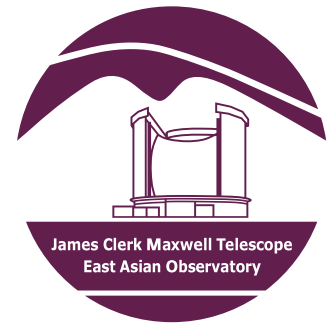


East Asian Observatory News

Issue #3, July 2017

In this Issue:

Director's Corner - P. Ho	3
New Large Programs - H. Parsons	4
JCMT: spying on Black Holes - R. Tilanu	5
The case of 252P - I. Coulson & M. Cordiner	7
The Transient Survey - S. Mairs & D. Johnstone.....	9
SCOPE - Tie Liu	12
The BISTRO Survey - K. Pattle & D. Ward-Thompson	14
The MALATANG Survey - T. Greve, Y. Gao, & Z. Zhang	16
JINGLE: an update - A. Saintonge	17
S2COSMOS - J. Simpson	19
STUIDES - W. Wang	21
The JCMT Ohana - aloha and a hui hou - H. Parsons	22



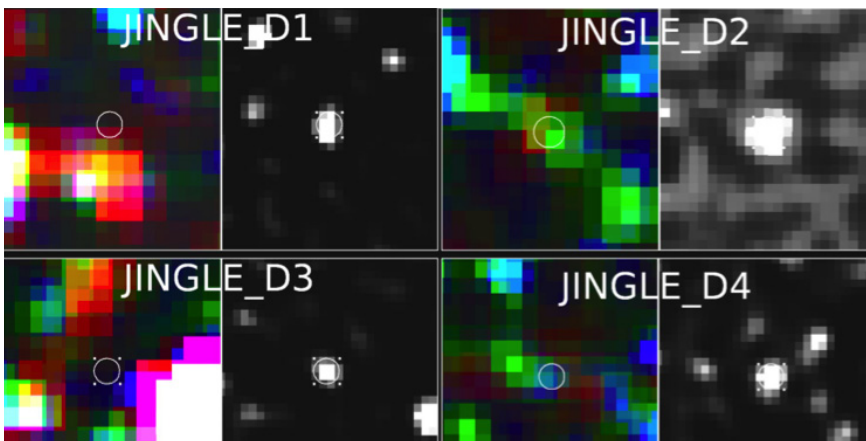
East Asian Observatory

660 North A'ohōkū Place
Hilo, Hawaii, 96720
USA

www.eaobservatory.org
helpdesk@eaobservatory.org

This copy of the East Asian Observatory News was produced and edited by Harriet Parsons and Iain Coulson. If you wish to submit an article for the next issue of the News please send an e-mail to:

newsletter@eaobservatory.org

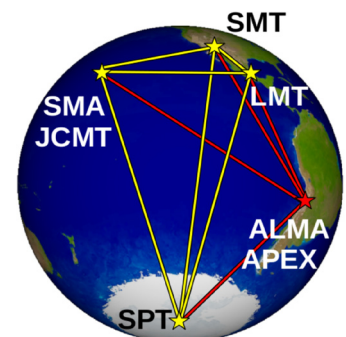


From the front cover.

Top: Four possible very distant and dusty galaxies surreptitiously detected by the JINGLE team. Left colour images are Herschel, Right in grey scale are SCUBA-2 850 micron.

Bottom Left: The EAO/JCMT staff outside the Hilo office.

Bottom Right: The Event Horizon Telescope including ALMA in 2017



Director's Corner

Paul Ho, Director General of EAO

The EAO is now in the third year of operations of the JCMT. The Observatory continues to operate smoothly and to deliver excellent science.

We have had six calls for PI proposals, and two calls for Large Programs. Proposal pressure continues to be high, with an over-subscription rate of ~3-5 across the partner regions. In the first call for Large Programs, seven projects were approved. Open enrollment into these approved projects resulted in some 230 new participants. More than half of the ~400 scientists involved in the large programs came from the new East Asian communities. Thanks to excellent weather in the 2016 winter, progress in the Large Programs has been swift, with three of the projects having acquired more than 70% of their data. Some of the initial papers have already been accepted for publication. We are also happy to report that the publication rate from the Observatory during the past two years remains at the historical rate of about 80 papers per year.

During April 2017, JCMT partici-

pated in the first Event Horizon Telescope experiment with the phased-up ALMA. This important experiment, to image the shadow of a supermassive black hole, is one of the key initiatives for JCMT on VLBI science. Successful fringes were confirmed in the early analysis of the data.

In terms of instrumentation, POL-2 is operating smoothly since the completion of commissioning. The resulting polarization maps are much deeper than the previous generation of SCUPOL results. We have installed new filters within SCUBA-2 ahead of the detectors. This has improved the sensitivity, and we are now studying the options for further improving the sensitivity. We are in the process of replacing RxA with a closed-cycle system. This will improve the sensitivity for VLBI experiments, and for the coverage of the 230GHz band.

In preparing for a successor to HARP, we are currently evaluating the possible technology of large format detectors. During the past year, JCMT held users meetings at NAOJ, Cardiff, and PMO. The next users meeting will

be held at KASI in Korea in January 2018. The Large Programs have also been holding team meetings across the regions, which have been very successful.

During the past year, the EAO has started to work on the SMA and Subaru, as additional facilities open to the EAO communities. East Asian regions were invited to apply for SMA time via ASIAA, starting with the 2017A semester. East Asian regions were also invited to apply for Subaru time during 2017A and 2017B semesters.

The EAO continues to engage the public via our various Outreach activities. Of particular note this year was the award of telescope time to a local school student Spencer Young from Kailani High School, on his project "Star forming regions and how they retain their shape" utilizing the POL-2 instrument. This was undertaken under the Maunakea scholars program which the JCMT is proud to support.

That is the news, and we look forward to our next update.



Figure 1. JCMT Users meeting, February 2017, Nanjing, China.

New Large Programs to build on success at the JCMT

Harriet Parsons, Large Program Manager, JCMT

The JCMT is pleased to announce that alongside the current set of Large Programs being undertaken by the JCMT, five new programs have been awarded time. In addition four existing programs have been awarded additional time to expand on their original scientific goals.

The observatory is dedicating 50% of science time through the end of Semester 19B to the Large Programs, in order to answer big science questions. The existing programs - those that began in December 2015 are already producing exciting science results. Some of these results are discussed in this edition of the Newsletter. However a few results have yet to be published and so the reader is encouraged to keep an eye out for JCMT publications over the coming months!

To date over 1,600 hours have been observed for the Large Programs. And the pressure is on. The JCMT Time Allocation Committee recently met in Hawaii to discuss both PI programs and

the new/extension requests for time under the Large Programs. The four extension requests are for STUDIES, BISTRO, JINGLE and S2COSMOS. These four programs are discussed later in this Newsletter.

The five newly approved programs are:

HASHTAG - the HARP and SCUBA-2 High-Resolution Terahertz Andromeda Galaxy Survey.

CHIMPS-2, a HARP program to map the inner Galactic Plane, the Central Molecular Zone and a section of the outer Plane in ^{12}CO , ^{13}CO and C^{18}O , extending the existing successful CHIMPS (Rigby et al., 2016) and COHRS surveys (Dempsey, Thomas and Currie 2013).

NESS - Nearby Evolved Stars Survey - targets a volume-limited sample of mass-losing AGB stars within 2 kpc of the Sun to derive the dust and gas return rates in the Solar Neighborhood, and constrain the physics underlying these processes.

S2XLS - SCUBA-2 Large eXtragalactic Survey will map 10 square degrees of extragalactic sky at $850\mu\text{m}$ to a depth of 2 mJy per beam. The survey will be split over two deep fields covered by the Subaru/Hyper Suprime-Cam (HSC) Survey: XMM-LSS and E-COSMOS.

NEP - the Extragalactic JCMT Survey of the North Ecliptic Pole with SCUBA-2.

For more information it is recommended the interested reader visit: www.eaobservatory.org/jcmt/science/large-programs/

It might be surprising to find so many programs in the queue. The result of awarding these programs is a large oversubscription in the Large Program Queue (by a factor ~two). The decision to oversubscribe has been made both due to the high quality of science proposals but also to provide flexibility - in terms of RA, instrument and weather - to the observatory.

A period of open enrollment has already occurred during which any eligible astronomer could join any of the Large Programs for which they feel they could contribute. Open enrollment in the Large Programs enables the observatory to promote and support new partnerships between the EAO communities.

With over 170 responses it is clear that the community is eager to engage in these new large science programs. We look forward to seeing some great science over the coming years.



Figure 2: The JCMT Time Allocation Committee at the EAO office in Hilo.

JCMT: spying on Black Holes

Remo Tilanus, EHT Project Manager, Leiden Observatory & Radboud University

In April 2017, almost 10 years to the day since it participated in groundbreaking observations that investigated the feasibility of the experiment, JCMT joined historical observations that are attempting to image the event horizon of a Black Hole. During a 10-day observing window the Event Horizon Telescope (EHT) together with ALMA carried out observations of Sgr A*, the supermassive black hole in the center of our own Galaxy, of a host of black holes in the centers of nearby galaxies, such as M 87 and Cen A, and of a number of well-known AGNs.

The EHT is a Very Long Baseline Interferometer (VLBI) array that observes at wavelengths of 1.3 mm (220 GHz) and, in the future, 0.87 mm (342 GHz). For the April observations the JCMT joined the SPT (South Pole), IRAM 30m telescope (Spain), APEX (Chile), LMT (Mexico), SMT (Arizona), and SMA (Maunakea), all of which have state-of-the-art wideband VLBI equipment that can accommodate an aggregate bandwidth of 8 GHz (32 Gb/s) i.e. dual-polarization 4 GHz bands.

Together, the EHT and ALMA make a VLBI array at 1.3 mm

with an unprecedented sensitivity and uv-coverage and the ability to actually resolve Sgr A*, opening the possibility of obtaining the first image ever of a black hole. The black hole is estimated to have a mass of 4 million M_{\odot} , and the silhouette or shadow of Sgr A*'s event horizon as seen from Earth is expected to be about 52 micro-arcsecs across, requiring world-spanning VLBI baselines. In addition to covering the peak of the non-thermal emission, submm frequencies are essential in order to penetrate scattering by matter close to the black hole.

This made the April VLBI campaign a long anticipated and high-stakes event. In preparation, the JCMT had upgraded its 230-GHz receiver with a new wideband mixer that increases the IF from a 2-GHz band to a range of 4-12 GHz. JCMT staff Per Friberg and Ken Brown together with Paul Yamaguchi (SMA) had done an excellent job in solving a number of lingering issues related to tuning and the stability of the new mixer and Ryan Berthold quickly fixed an unanticipated software issue that popped up during the final tests. Three days before the start of observing, local 'fringes' with

the SMA could be confirmed.

In this 'eSMA' mode JCMT joins the SMA interferometer, mimicking one of its antennas, which allows for a comprehensive end-to-end test of the system. This test was also performed prior to each VLBI observing night. Note however that during the observations itself JCMT is a separate VLBI station on Maunakea.

Having verified the technical readiness of the JCMT, the focus next shifted to weather. After all, it is no mean feat to have good or acceptable weather at six locations around the world. Fortunately, the weather cooperated and was good, and exceptional at some of the sites, for a period of a week.

Consequently, 1.3 mm VLBI commenced on the first day of the observing window, April 4 HST. Day 4 and 5 were skipped due to high winds at the SMT and the threat of ice at the LMT, before observations were completed on day 6 and 7, after which Maunakea experienced several days of bad weather.

The availability of a custom long-term water vapor forecast for each of the sites through

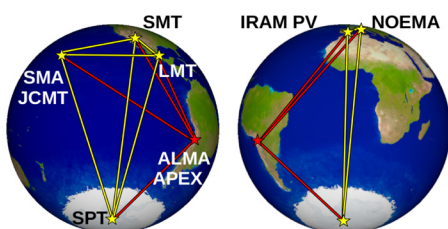


Figure 3: The Event Horizon Telescope and ALMA in 2017, as seen from Sgr A* (NOEMA did not participate).

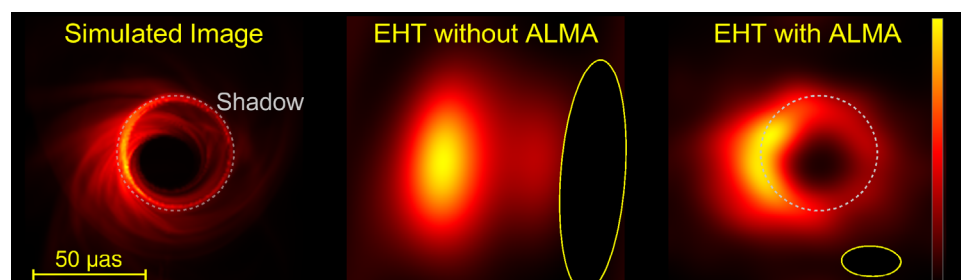


Figure 4: Imaging the Shadow of a Black Hole. The figure shows a model image from a numerical simulation of SgrA*. The image is bright on the approaching side of the accretion disk and faint on the receding side because of Doppler effects. Figure 3: The left and right panels show simulated images from the EHT without and with ALMA.

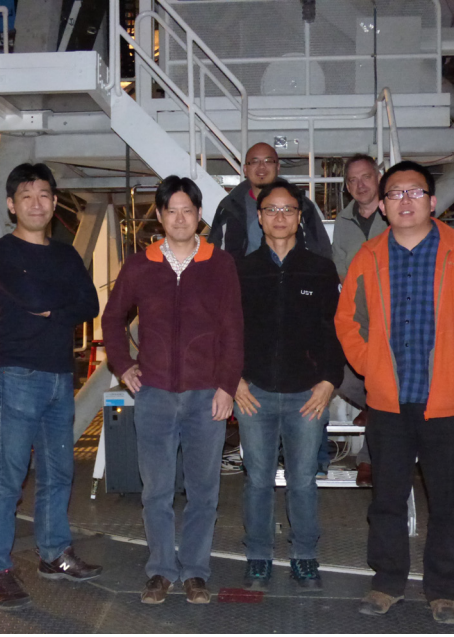


Figure 5: Sleep-deprived JCMT VLBI observers. From left: Satoki Matshushita (ASIAA), Mareki Honma (NOAJ), Kevin Koay (ASIAA), Taehyun Jung (KASI), Remo Tilanus (Leiden Obs & Radboud Un.), Feng Gao (SHAO).

EHT's VLBI monitor and courtesy of the Royal Netherlands Meteorological Services proved to be extremely helpful, even in a non-optimized form. Another very useful addition to this year's observing was establishing a non-oxygen-deprived EHT operations center in Cambridge (MA) for the daily go/no-go decision and coordination of any fault response. The final night was used to make up for time lost due to technical faults at a few sites, the most severe one due to a power failure and lasting for more than 4 hours. Many of the targets received close to their allocated integration time.

Due to the length of the nightly schedules, many sites operated with two crews. In addition, the JCMT rotated some of the crew mid-way through the ob-

serving window. This made for a crowded control room. But not for nothing: while it is too early to say anything about the scientific results, preliminary checks have confirmed fringes between all telescopes, except SPT (data stuck at SP until November) and APEX (data still in transit). Figure 6 shows a very strong fringe on 3C279 between JCMT and ALMA

A number of other observatories carried out concurrent observations of Sgr A* and M87 during the VLBI campaign. This is illustrated in figure 7. Especially note the two observed flare events: if detectable in the VLBI observations as a time-variable closure-triangle signal it may provide a straightforward measure of the spin of Sgr A*.

In summary: the first EHT-ALMA VLBI campaign went about as well as one could have expected, without any major technical showstoppers or significant impact from weather. Based on a very quick preliminary check the observations look of good quality and great promise.

On behalf of the VLBI team we sincerely thank the staff of the JCMT for their support of these logistically challenging observations. Special thanks go to JCMT's telescope operators, Jim Hoge, William Montgomerie, and Kevin Silva, for their hard work and professional care in manually executing the VLBI schedule.

Remo Tilanus acknowledges support from the Netherlands Organization for Scientific Research (NWO) and from the ERC Synergy Grant "BlackHoleCam - Imaging the Event Horizon of Black Holes" (Grant 610058).

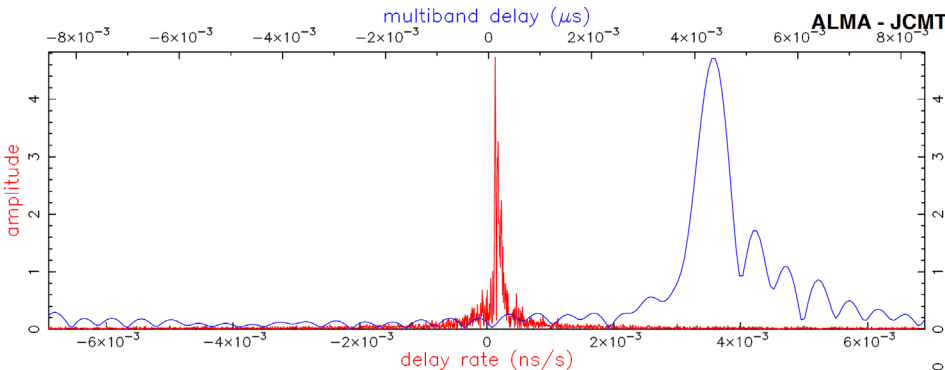


Figure 6: Strong fringe in April 2017 on 3C279 on the JCMT-ALMA baseline. The red line shows a peak in delay-space with a S/N of over 500.

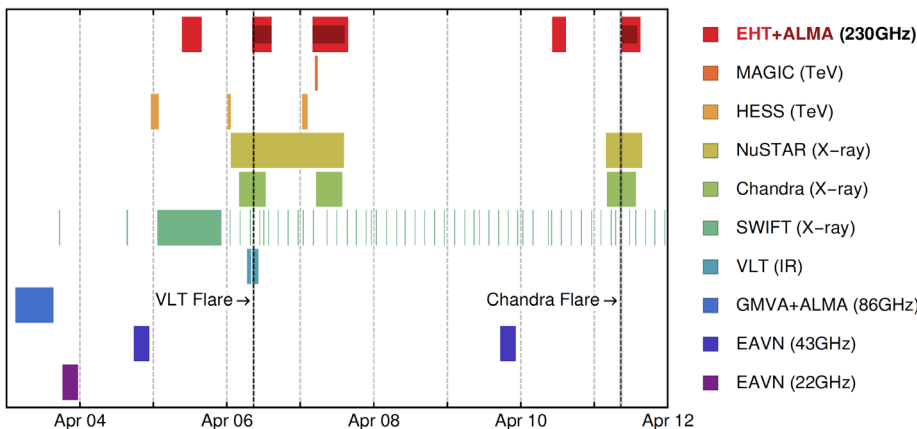


Figure 7: Concurrent multi-wavelength observations of Sgr A* during EHT-ALMA VLBI.

On the Origin of (cometary, molecular) Species** ; the case of 252P

Iain Coulson and Martin Cordiner

Comets are often described as pristine relics from the early Solar Nebula and promise to reveal the physics and chemistry of that nebula - if only we could link their origins, via their environmental history, to their current characteristics. Dynamical considerations recognize that the Oort Cloud comets, for instance, arose in the same region of the nebula where the giant planets formed, while the origin of the Jupiter Family comets is likely to be the more distant Edgeworth-Kuiper belt. We have run a comet observing campaign from JCMT for many years, targeting comets of any type whenever their apparitions were favourable, in an attempt to elucidate their chemical characteristics. Comets are notoriously unpredictable, so we must make best use of each opportunity.

The Jupiter Family comet 252P

(LINEAR) passed the Earth at a distance of 0.035 AU on 21st March 2016, presenting a rare opportunity to study a comet with JCMT at relatively high spatial resolution. In 7 nights of observing starting on 27th March, we(*) observed 252P using both SCUBA-2, with which we obtained continuum images, and estimated the production rate of dust particles with size ~ 1 mm to be 4 kg/s, and HARP, with which we detected several molecular species.

The proximity of the comet offered the chance to spatially resolve the processes occurring in the inner coma, and to inform the debate about the origin of each molecular species; be it 'primary', i.e. emerging directly from the nucleus, or 'extended', i.e. resulting from the thermal or photochemical processes that affect the primary species once exposed to

the solar radiation field.

The strongest submillimeter emission from comets is typically that from hydrogen cyanide (HCN), and the J=4-3 transition at 354 GHz from 252P was strong enough to allow us to make HARP jiggle maps of the inner coma at a resolution as small as 500 km, in the plane of the sky. This resolution degraded to 850 km by the end of our observing week, but the resolution was sufficient to show the HCN emerging from a fairly compact, cometocentric region of FWHM 960 km, and consistent with HCN being a primary species.

The emission lines vary in pro-

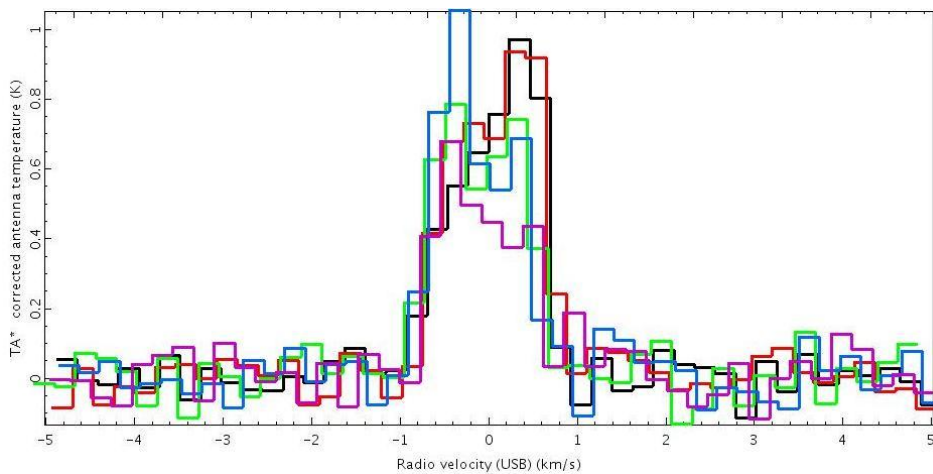


Figure 8. HCN J=4-3 (354.5055 GHz) line profiles of comet 252P on March 27th (UT). Spectra are corrected for the radial velocity of the comet nucleus as provided by the JPL/Horizons ephemeris, and displayed in the cometocentric velocity frame at a channel spacing of 0.25 km s^{-1} . The temperature scale is TA^* . Colors and UT dates are as follows: Black (2016-03-27.56, Red 27.58, Green 27.65, Blue 27.71, Purple 27.75.

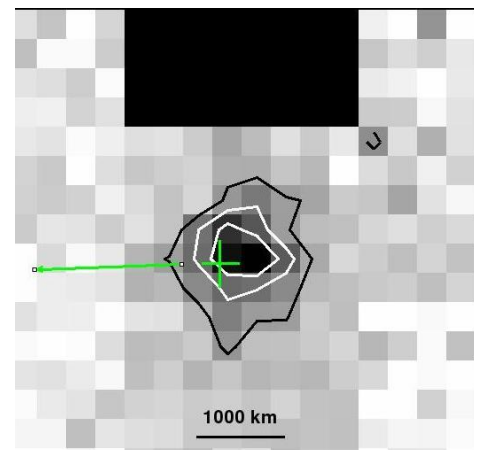


Figure 9. Integrated brightness of the seven strongest methanol lines from jiggle maps of 252P taken with HARP on March 28th & 29th. North is up; East left. The pixel size is $7.5''$, and the HARP footprint is $2'$ across. The expected position of the comet nucleus on the 29th is marked by the green cross. The green vector shows the direction to the Sun. The contours show 40% (black), 60% (white) and 80% (white) of peak intensity.

file on hour-long timescales (Fig. 8), but in a way inconsistent with a varying perspective on a single jet leaving a rotating nucleus, and more likely indicative of variations in the rate of outgassing from the nucleus. This might be due either to sporadic jet activity or to variations in the size of the active surface, caused by inhomogeneity of the nucleus. Nonetheless, the overall activity level was reasonably stable throughout the week, with the rate of HCN production being a rather modest $(6.4 \pm 1.0) \times 10^{24}$ mols/s. Independent, contemporaneous estimates of the production rate of water of $(4.5 \pm 1.0) \times 10^{27}$ mols/s (156 kg/s) yield a HCN:H₂O ratio for 252P of 0.12%, which is within the range seen in other comets (0.08-0.30%). The produc-

tion rates of water and dust also indicate that, on the scale between dirty-snowball and snowy-dirtball, 252P is one of the least dirty comets ever observed.

We were also able to make maps of 252P in several of the 338 GHz emission lines of methanol, and the resulting intensity map (Fig. 9) is again compact and cometocentric. Such data are suitable for analysis for gas temperature and density by application of an improved version of the traditional rotational diagram method - the 'Zero Gradient' method. Similar analysis of ALMA data of comet C/2012 K1 (PanSTARRS) showed methanol to be a primary species, so it was a surprise that, by contrast, analysis of our data for 252P showed

that the best fitting temperature and density profiles require that methanol be considered as an extended species - see the 'Daughter Model' fit in Fig. 10, derived assuming, unrealistically, the conversion to methanol of some primary (parent) species. It is more realistic that the methanol in the coma of 252P is a primary species and is released by sublimation from a population of icy grains - an "ice halo" - surrounding and expanding from the nucleus. Sublimation from such grains, and on very similar scale lengths, was previously suggested as the source of the water and HCN from comet 103P (Hartley-2). It is feasible that all the gases from 252P may originate from the sublimation of icy grains in the coma. Whether such mechanisms are common will require similar observations of many more comets of different types.

* This article is a summary of a paper which appears in the *Astronomical Journal*, Vol 153, p169. Our colleagues are Stefanie Milam and Steven Charnley at Goddard Space Flight Center, Yi-Jehng Kuan, Wei-Ling Tseng, and Yo-Ling Chuang at NTNU, and Zhong-Yi Lin and Wing-Huen Ip at NCU in Taiwan.

** with apologies to C.Darwin

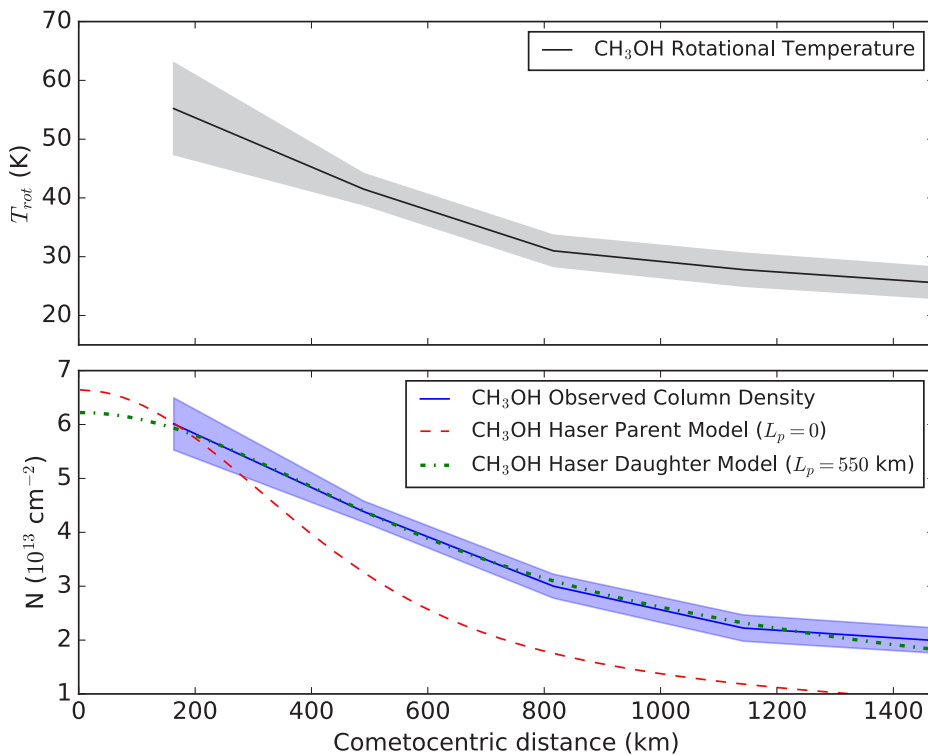


Figure. 10.— Azimuthally averaged rotational temperature and column density profiles derived from methanol (338 GHz) spectra of comet 252P on March 29th. Haser-type model fits to the observed column density profile are shown assuming methanol both as a primary species (shown as 'parent' in the legend) and as an extended ('daughter') species with a parent scale-length of 550 km.

The Transient Survey: Advances in Spatially Aligning and Flux Calibrating SCUBA-2 Images

Steve Mairs, Doug Johnstone, and the Transient Team

The JCMT Transient Survey (Herczeg et al., in preparation) is a three-year project dedicated to observing variability in deeply embedded protostars at submillimetre wavelengths with SCUBA-2. With a monthly cadence, we monitor eight star-forming regions, selected from the JCMT Gould Belt Survey (Ward-Thompson et al., 2007) that have a high density of known protostellar

and disk sources (Young Stellar Object Classes 0 to II).

In order to accurately track the peak brightness of these submillimetre sources across epochs, we employ a robust data reduction method, using multiple observations of the same regions to derive post-reduction image alignment, and using relative flux calibration techniques (Mairs et al. submitted). As such, we are able to significantly improve on the nominal JCMT pointing uncertainty of 2-6" ($1-3\sigma$) and flux calibration uncertainty of, at least, 5 to 10% (Dempsey et al. 2013).

The first requirement for effective relative calibration is a

well-defined and appropriate data reduction and map-making strategy. Following the approach of Mairs et al. (2015) we considered four different map-maker set-ups, applying a spatial filter to structures larger than either 200" or 600" and performing map reconstructions with or without external masks. The 200" filter, coupled with an external mask, is found to produce the best results for the Transient survey, since we are mostly interested in compact emission peaks. The other three set-ups also work and yield consistent relative alignment and flux calibration factors, providing additional confidence in our results.

To align and flux calibrate the individual maps we first produce source catalogues of the localized emission, employing the Gaussclumps algorithm (Stutzki & Guesten 1990) as implemented in the Starlink package CUPID (Berry et al. 2007). The advantage of Gaussclumps over other publicly available source-

finding algorithms is that by fitting a constrained Gaussian to each emission peak, we can accurately determine the peak location and peak brightness of all the compact sources in a given map while performing a subtraction of larger-scale background flux. The location and

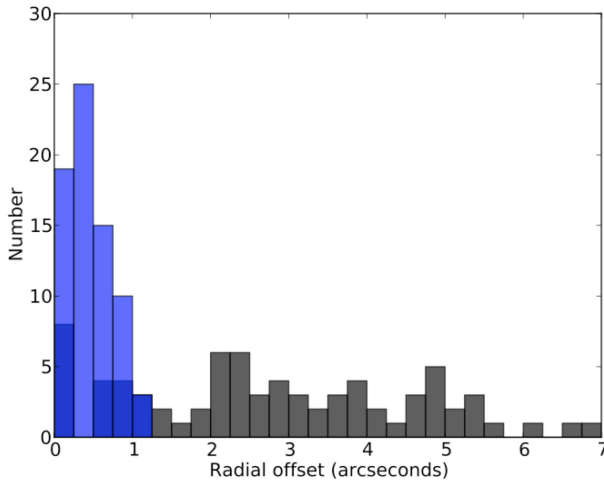


Figure 11. Histograms of the measured radial offset between each region's reference field and its subsequent observations. Black represents the original offset without applying any correction; blue represents the corrected offset of the aligned maps. [Figure adapted from Mairs et al. submitted]

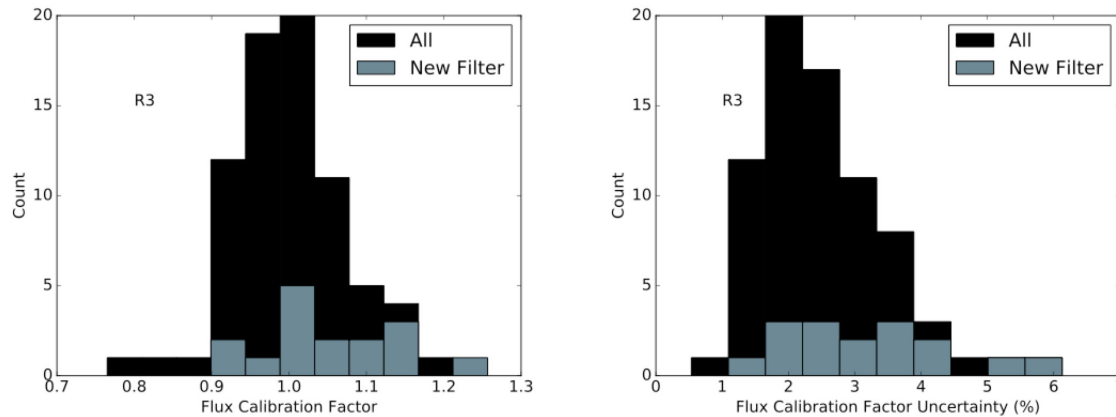


Figure 12. Left panel: The required flux calibration factor applied to each observation to bring the regions to a common relative calibration. Right panel: The uncertainty in the calibration factor for each observation as measured directly from the sources in the region. The grey boxes indicate observations taken after the filter change in November, 2016. [Figure adapted from Mairs et al. submitted]

brightness are precisely the quantities that we are most interested in obtaining in order to perform these post-reduction calibrations. Nevertheless, given that sub-millimetre sources are seldom point-like or Gaussian, we anticipate a non-negligible residual in these fit parameters whenever the source becomes complex or resides in a complicated region. To mitigate this somewhat, we only use those Gaussian sources for which the peak brightness is greater than 200 mJy/bm and the derived FWHM is less than 20".

To determine the telescope alignment offset between epochs, we identify the first observation as the reference frame and match the source cata-

logues between the reference frame and the observation of interest. We take the alignment offset to be the mean RA and Declination offset between the two catalogues. Figure 11 shows the telescope radial alignment offset between all Transient observations and their respective reference frames (black histogram).

We next re-reduce the SCUBA-2 observation, applying these measured offsets during the map-making procedure to produce a final aligned map gridded identically as the reference frame. As a check, the Gaussclumps output for this re-reduced map is compared against the reference frame source list to determine the re-

sidual alignment offset. Figure 11 shows that the residual radial offset is less than $\sim 1''$ (blue histogram), substantially smaller than an individual 850 μ m map pixel (3").

The entire process of data reduction and alignment is accomplished automatically through a scripting process at EAO (many thanks to EAO staff Sarah Graves and Graham Bell) and the aligned images are deposited in the appropriate Transient VOSpace folder at the CADC for relative flux calibration analysis and use by the Transient team.

After cataloguing all epochs for a given region, we derive and apply a relative flux calibration factor to each observation in order to plot accurately the brightness variations of a given object over all epochs. The error on the intrinsic absolute flux calibration of SCUBA-2 850 μ m measures at JCMT is $\sim 5\text{-}10\%$ (Dempsey et al. 2013), but we are focused only on the relative brightness changes from epoch to epoch. This allows us to achieve more accurate measurements of the variability in a given field. The procedure to flux calibrate our images consists of three steps:

- 1) Using only the brightest (>500 mJy/bm) sources, for which the intrinsic signal to noise in the map is > 50 , we determine the flux ratios for all pairs of sources across all epochs. By taking this ratio, we disentangle the initial map calibration and calibration uncertainties from the determination of appropriate calibration sources.

- 2) We measure the scatter in the flux ratios for each pairing across all epochs as a way to

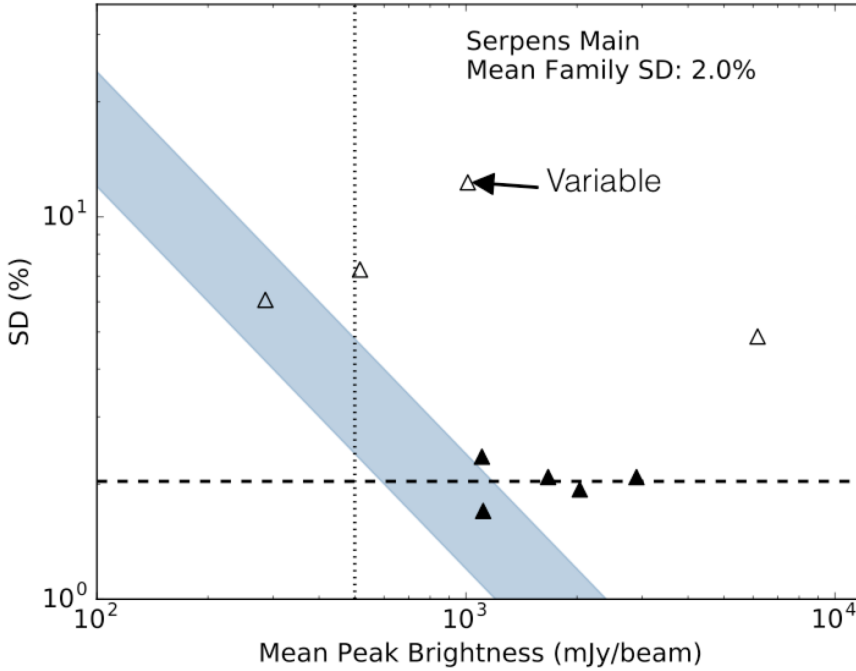


Figure 13. The standard deviation in the peak brightness versus the mean peak brightness of a source in the Serpens Main Transient field. Filled triangles represent the subset of sources used for the flux calibration while empty triangles represent sources not included in the flux calibration. The vertical dotted line indicates the minimum brightness threshold to be considered a flux calibrator. The horizontal dashed line shows the average standard deviation in the mean peak brightness of all the flux calibrators. The lower bound of the shaded region shows the average noise as a percentage of source peak brightness and the upper bound of the shaded region assumes the noise is higher by a factor of two. [Figure adapted from Mairs et al. submitted].

determine which sources are intrinsically stable. A ‘Family’ of ‘non-varying’ sources is found by imposing the constraint that all non-varying sources must satisfy a small scatter ($< 6\%$) constraint against each other. Sources omitted from the Family are either varying sources or sources with more complicated structure, making determination of their peak flux less reliable.

3) For each epoch, the relative flux calibration factor is derived from the average normalised peak brightness over all the sources in the Family during that observation. These factors are plotted in the left panel of Figure 12. The uncertainty in the flux calibration factor is determined from the standard deviation of the normalized peak brightness of all the calibrator sources. This uncertainty is plotted in the right panel of Figure 12.

The highest flux calibration factor uncertainties are for the NGC2024 region where our Gaussian fitting routine encounters more uncertainty in fitting peaks due to the complex structure. Overall, the flux calibration uncertainties are very low, 2-3%, allowing the JCMT Transient Survey team to robustly detect variations in peak brightness to

the level of $\sim 10\%$. Presently, we are working to automate the flux calibration procedure such that it can also be run directly after an observation undergoes the data reduction and alignment procedures at the EAO.

In Figure 13, we plot both the measured fractional variation for each source in Serpens Main over all epochs (ordered by peak brightness). For a source to be included in such a plot, it must be detected in every epoch of the given region. Thus, there are many additional, potentially interesting, submillimetre sources that are not included in these figures but will be investigated more closely by individuals within the specific Transient Region Team. The five dark triangles in Figure 13 denote the Family of sources used to calculate the relative flux calibration in the Serpens main field. Note, however, that all plotted sources are used for the alignment calibration. In Figure 14 we show the measured, normalised source brightness as a function of epoch for two reference sources.

The primary goal of the JCMT Transient Survey is to detect variability in the brightness of deeply embedded protostars over a three-year window. The

enhanced alignment and flux calibration schemes that we have developed allow detailed investigations by team members associated with individual regions using several techniques including image blinking, image subtraction, and a variety of clump-finding analyses. The labeled unfilled triangle in Figure 3 (top panel) marks the first robust submillimetre variable source uncovered by the Transient Survey (Yoo et al. in preparation). Stay tuned for more about this source.

For further information on the alignment and calibration, please contact the authors or read the full calibration paper (Mairs et al. submitted).

References

- Berry D. S., et al., 2007, *Astronomical Society of the Pacific Conference Series Vol. 376, Astronomical Data Analysis Software and Systems XVI*. p. 425
 Dempsey J. T., et al., 2013, *MNRAS*, 430, 2534
 Mairs S., et al., 2015, *MNRAS*, 454, 2557
 Stutzki J., Guesten R., 1990, *ApJ*, 356, 513
 Ward-Thompson D., et al., 2007, *PASP*, 119, 855

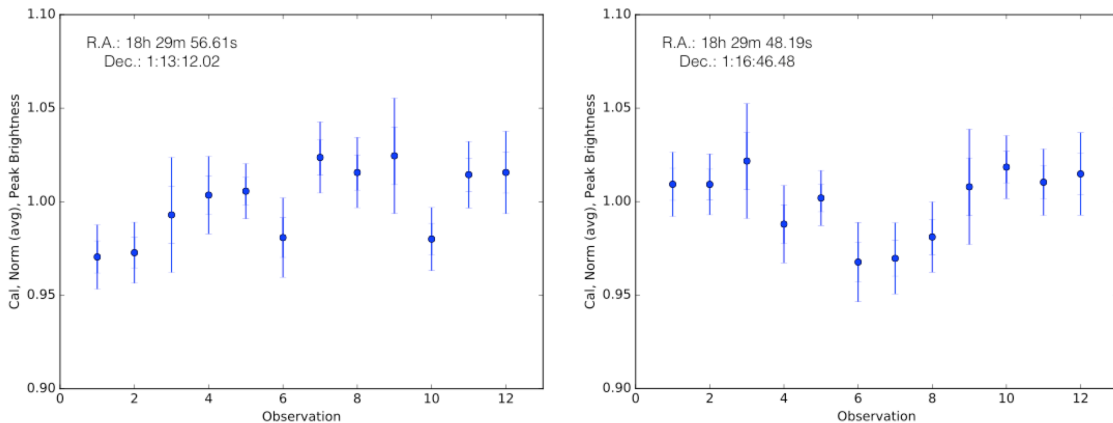


Figure 14. Normalized flux versus epoch for two of the five sources used for relative calibration of Serpens Main.

SCOPE: SCUBA-2 Continuum

Observations of Pre-protostellar Evolution

Tie Liu on behalf of the TOP-SCOPE team.

The Planck team has identified 13188 Planck Galactic Cold Clumps (PGCCs). The PGCC catalogue, covering the whole sky, hence probing wildly different environments, represents a real goldmine for investigations of the early phases of star formation (Planck collaboration et al. 2015). Toward this end, we have been carrying out a legacy survey toward 1000 PGCCs with JCMT/SCUBA-2 in 850 micron continuum, "SCOPE: SCUBA-2 Continuum Observations of Pre-protostellar Evolution". The project is now ~80% complete. Thousands of dense cores have been identified in the "SCOPE" survey, and most of them are either pre-stellar cores or very young (Class 0/I) protostellar objects. They are thus prime candidates for probing the very initial stages of star formation in a wide variety of Galactic environments. We have formed a technical team to reduce the data and extract compact cores. To promote

collaborations, we held the first SCOPE workshop in December at Peking University, Beijing. About 50 participants attended the workshop.

In conjunction with our joint surveys at other observatories (e.g., KVN 21-m, NRO 45-m, TRAO 14-m and SMT 10-m), we are carrying out comprehensive studies on the topics related to the initial conditions of star formation. Below we present three examples of our studies:

1. Extremely cold, quiescent and massive filaments

Herschel surveys have revealed universal filamentary structures in molecular clouds, suggesting that stars prefer to form in dense filaments. The SCOPE survey has provided us dozens of extremely cold, quiescent and massive filaments, which may represent the very initial conditions for high-mass star formation. In Figure 15,

we present such a filament, the coldest core in which is as cold as ~8 K.

2. Stellar feedback on star formation

We are statistically investigating the effect of stellar feedback on star formation by investigating the PGCCs located near HII regions (e.g., Lambda Orionis complex, see left panel of Figure 16). We found the dense core detection rate of PGCCs at 850 micron in the Lambda Orionis cloud (16%, 8 out of 50) is much smaller than in Orion A (76 %; 23 out of 30) and Orion B (56%; 9 out of 16). In addition, the dense cores in the Lambda Orionis complex show much smaller density, mass and dense gas fraction than the dense cores in Orion A and Orion B. Therefore, we argue that stellar feedback may have very negative effects on core (or star) formation (Yi et al. 2017, in preparation).

In the Lambda Orionis complex, we identified 8 Class 0/I protostellar cores from the SCOPE survey - see Figure 16. These 8 cores are really interesting for studies of the initial conditions of star formation under the influence of stellar feedback (e.g., radiation, stellar wind) from HII regions. The SMA follow-up observations of these 8 cores have been conducted. We also submitted an ALMA cycle 5 proposal in order to investigate their properties in detail.

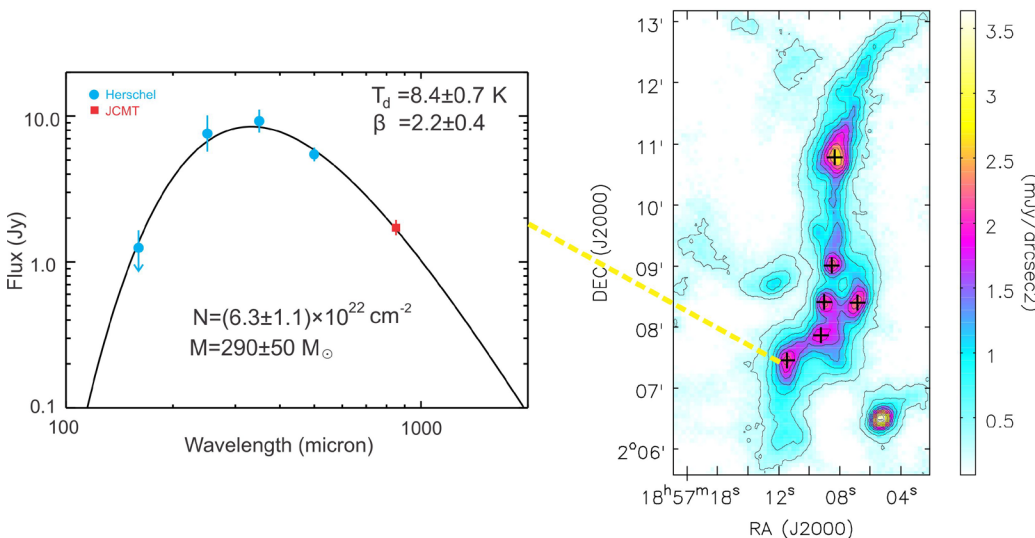


Figure 15. Left panel: the SED of a cold core. Right panel: the SCUBA-2 850 micron continuum image of a cold, quiescent and massive filament.

3. Cloud-Cloud collisions

Cloud-cloud collisions can enhance star formation and also form filamentary structures, as revealed in simulations (e.g., Haworth et al. 2015, MNRAS, 450, 10; Wu et al. 2016, arXiv160601320W). However, the evidence for cloud-cloud collision

is hard to detect from observations. Our SCOPE and joint surveys toward Planck cold clumps (e.g., G178.2, see Figure 17) clearly indicate that filaments can be formed through cloud-cloud collisions. As shown in the left panel of Figure 17, two clouds with very different velocities seem to collide with each other and greatly enhanced density appears at the interface. At the

colliding interface, a S-shaped dense filament, which is highly fragmented, is detected in the 850 micron continuum (right panel). Young stars are forming inside the S-shaped filament. The observations of G178.2 clearly suggest that large-scale cloud-cloud collisions can form filaments and enhance star forming activities at the interface (Zhang et al. 2017, in preparation).

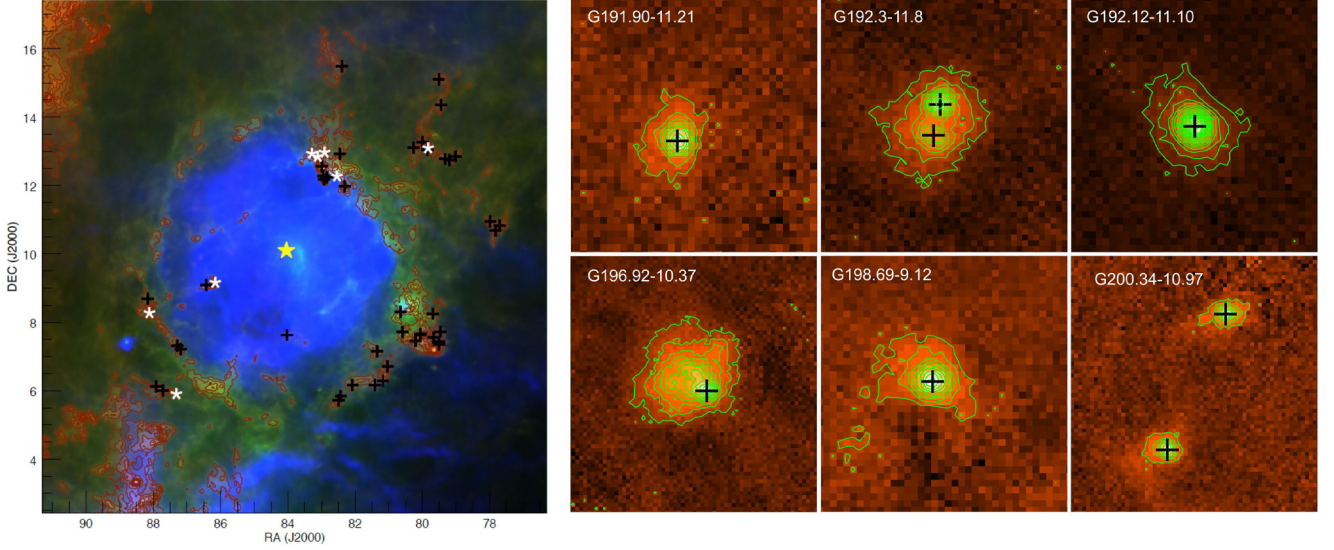


Figure 16. Left panel: Three-color composite image (red: Planck 353 GHz; green: IRAS 100 micron; blue: H α) of the Lambda Orionis complex. The red contours show the flux density of Planck 353 GHz. The yellow star represents “Lambda Ori” OB star association and black crosses are dense PGCCs. The white “*” mark the PGCCs with SCUBA-2 detection. Right Panels: JCMT/SCUBA-2 850 micron continuum of PGCCs in the Lambda Orionis molecular complex. The black crosses mark the Class 0/I Young Stellar Objects (Yi et al. 2017, in preparation).

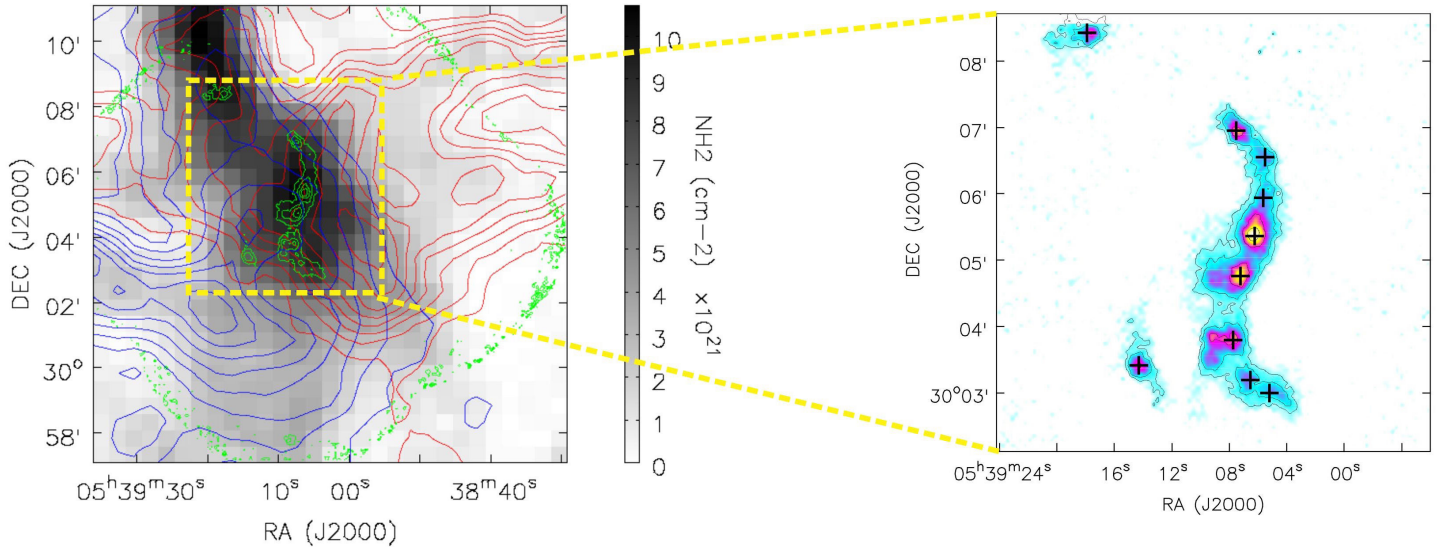


Figure 17. Left panel: The grey image shows the column density map of G178.2. The red and blue contours represent the 12CO (1-0) integrated intensity maps of the two colliding clouds. The green contours show in the 850 micron continuum. Right panel: The highly fragmented S-shaped filament as seen in SCUBA-2 850 micron continuum.

The BISTRO Survey: early results on Orion A

Kate Pattle and Derek Ward-Thompson on behalf of the BISTRO survey

The BISTRO survey has for the last year been mapping the Gould Belt in polarised light. The maps that have been produced as a result are unprecedented both in their depth and in the wealth of detailed magnetic field structure that they show. These data will allow detailed analysis of the interaction between magnetic fields and cores, filaments and outflows in a wide variety of environments. Early results from observations taken toward the OMC 1 region of Orion A show a wide variety of relationships between magnetic field geometry and gas distribution within a single star-forming region. Most notably, we see an hourglass-shaped magnetic

field extending from the centre of the integral filament into the lower-density surrounding material (Ward-Thompson et al. 2017).

The Orion A molecular cloud is a well-resolved and well-studied region of high-mass star formation (e.g. O'Dell et al. 2008), located relatively close to the Solar System, at a distance of 388 ± 5 pc (Kounkel et al. 2017). The dominant feature in dust continuum observations of Orion A is the 'integral filament' (Bally et al. 1987), a high-mass star-forming filament which runs north/south through our field (Figure 18). Our observations are centred on the OMC 1 sub-region, which is host to the mas-

self-gravitating filaments (e.g. Nakamura & Li 2008). Moreover, these observations are consistent with a recently-proposed paradigm of star formation in which clouds first collapse along magnetic field lines to form filaments, before the filaments become gravitationally unstable and fragment to form star-forming cores (André et al. 2014).

Other magnetic field behaviours are also seen in OMC 1. A filament in the north-eastern region of OMC 1 (labelled in Figure 18) shows magnetic field vectors running parallel, rather than perpendicular, to the filament direction. The polarisation structure in this region is shown in detail in Figure 19. The magnetic field in this region appears to cut through the hourglass field associated with the OMC 1 region, leading us to speculate that the north-eastern filament may lie in the foreground of OMC 1. Our observations suggest that this filament is not self-gravitating, as magnetic field lines running parallel to the filament is characteristic behaviour for a non-self-gravitating filament (e.g. Falceta-Gonçalves et al. 2008).

Along the centre of the integral filament the magnetic field lies approximately perpendicular to the filament, with a relative angle of $75^\circ \pm 7^\circ$. This is consistent with previous observations of the magnetic field structure surrounding self-gravitating filaments (e.g. B. Matthews et al. 2001; Palmeirim et al. 2013; T. Matthews et al. 2014), and with simulations of magnetised

The two different behaviours that we see in the integral and north-eastern filaments are consistent with simulations performed by Soler et al. (2013), who investigated the behaviour of magnetic fields in filaments as a function of magnetic field strength and filament volume density. They found that there is a critical volume density above which magnetic fields lie perpendicular to the filament, and below which they lie parallel to the filament. Our results suggest that we see

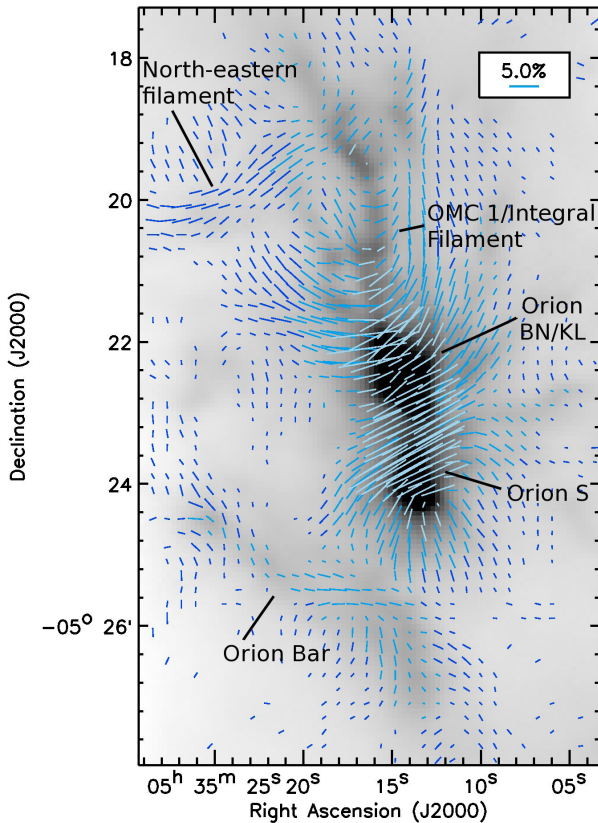


Figure 18: A magnetic field map of OMC 1, with polarisation half-vectors rotated by 90° to trace the magnetic field. The underlying image is an $850\mu\text{m}$ SCUBA-2 image of the same region. Vectors with $P/DP > 3$ are shown. Adapted from Ward-Thompson et al. (2017).

filaments both above and below this critical density in OMC 1. Soler et al. (2013) find that high magnetic field strengths are required for field lines to lie perpendicular to filaments, even above the density threshold, suggesting that the magnetic field strength in OMC 1 is high.

While the overall behaviour of the magnetic field strength in OMC 1 is consistent with the paradigm of magnetically-regulated filament formation, there are clearly features in the magnetic field which are not explained using this simple model, most notably the hourglass morphology of the OMC 1 region.

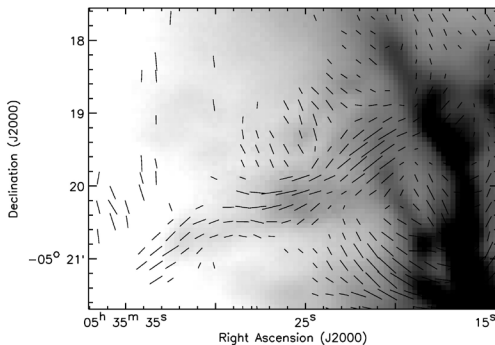


Figure 19: The polarisation structure of the north-eastern filament as observed with POL-2 (half-vectors rotated by 90° to trace magnetic field). From Ward-Thompson et al. (2017).

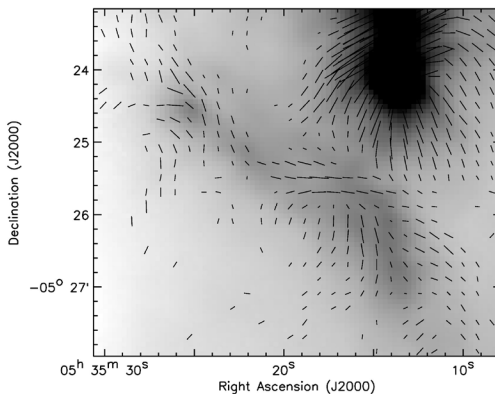


Figure 20: The polarisation structure of the Orion Bar as observed with POL-2 (half-vectors rotated by 90° to trace magnetic field). From Ward-Thompson et al. (2017).

Away from the centre of the filament, the magnetic field shows large-scale, highly-ordered deviation from cylindrical symmetry. The hourglass field morphology (c.f. Schleuning 1998; Rao et al. 1998) is suggestive of the magnetic field being distorted from an initially cylindrically-symmetric morphology. Possible candidates for the cause of this distortion, namely gravitational interaction of the BN/KL and S clumps and/or the effects of the highly energetic BN/KL outflow (Thaddeus et al. 1972; Allen & Burton 1993), are considered in detail by Pattle et al. (2017, ApJ submitted).

The Orion Bar also shows a potentially complex field morphology, as shown in Figure 20. Our observations are consistent with a scenario in which the magnetic field is simply following the PDR front, in a manner similar to a magnetic field running parallel to the direction of a non-self-gravitating filament. However, the observations are also consistent with the Orion Bar being wrapped by a helical magnetic field (e.g. Franzmann & Fiege 2017). In this case, interpretation of the magnetic field which we observe, which is a three-dimensional structure projected onto the plane of the sky, is complicated by the fact that we view the Orion Bar edge-on (Tielens et al. 1993), and so see the magnetic field integrated through the length of the PDR. Understanding the role of the magnetic field in the Orion Bar will require detailed modelling and will be the subject of a future study.

The BISTRO POL-2 map of the OMC 1 region shows a spectacularly detailed and com-

plex physical picture. Our initial studies show both large-scale magnetic field behaviour consistent with current paradigms of filamentary star formation (Ward-Thompson et al. 2017), and a region in which magnetic fields, gravity and outflows interact in a complex and highly energetic environment (Pattle et al. 2017, *subm.*). There is a wealth of information to be gained and a wide variety of physical environments to be studied in this single field. The BISTRO survey's ongoing mapping of the Gould Belt in polarised light will allow us to perform similar analyses in many nearby star-forming clouds, many of which are vastly different environments to anything found in Orion A. Extending our preliminary studies to investigate the roles of magnetic fields in high- and low-mass, star-forming regions will provide a vital piece of the puzzle of star formation.

References

- Allen & Burton 1993, *Nature* 363 54
- André et al. 2014, *Protostars and Planets VI*, p. 27
- Bally et al. 1987, *ApJL* 312 L45
- Falceta-Gonçalves et al. 2008, *ApJ* 679 537
- Franzmann & Fiege 2017, *MNRAS* 466 4592
- Kounkel et al. 2017, *ApJ* 535 887
- Matthews, B. et al. 2001, *ApJ* 562 400
- Matthews, T. et al. 2014, *ApJ* 784 116
- O'Dell et al. 2008, *Handbook of Star-Forming Regions, Vol. I*, p. 544
- Nakamura & Li 2008, *ApJ* 687 354
- Palmeirim et al. 2013, *A&A* 550 A38
- Pattle et al. 2017, *ApJ* submitted
- Rao et al. 1998, *ApJL* 502 L75
- Schleuning 1998, *ApJ* 493 811
- Soler et al. 2013, *ApJ* 774 128
- Thaddeus et al. 1972, *ApJL* 176 L73
- Tielens et al. 1993, *Science* 262 86
- Ward-Thompson et al. 2017, *ApJ* accepted, arXiv:1704.08552

The MALATANG Survey of dense gas in nearby galaxies

Thomas Greve, Yu Gao, and Zhiyu-Zhang on behalf of the MALATANG team

MALATANG was approved as one of seven large programs on the JCMT in 2016. The survey utilises the 350GHz heterodyne array HARP to map the HCN and HCO⁺ J = 4 - 3 line emission in 23 of the nearest IR-brightest galaxies beyond the Local Group. The aim is to map the distribution of dense ($\sim 10^4 \text{ cm}^{-3}$) gas in these galaxies on sub-kilo-par-

sec scales ($\sim 0.2 - 2.8 \text{ kpc}$) out to significant galactocentric distances. MALATANG bridges the gap in physical scale and luminosity between extragalactic (i.e., galaxy-integrated) and Galactic (i.e., single molecular clouds) observations. An important outcome of the survey will be a characterization of the distributed dense gas star-forma-

tion relations, as traced by the HCN and HCO⁺ J = 4 - 3, across our targets. From low surface density environments in disks to nuclear regions where surface densities are high, MALATANG will yield new insight into whether such environments harbour fundamentally different star-formation modes and efficiencies. The fact that this will be done

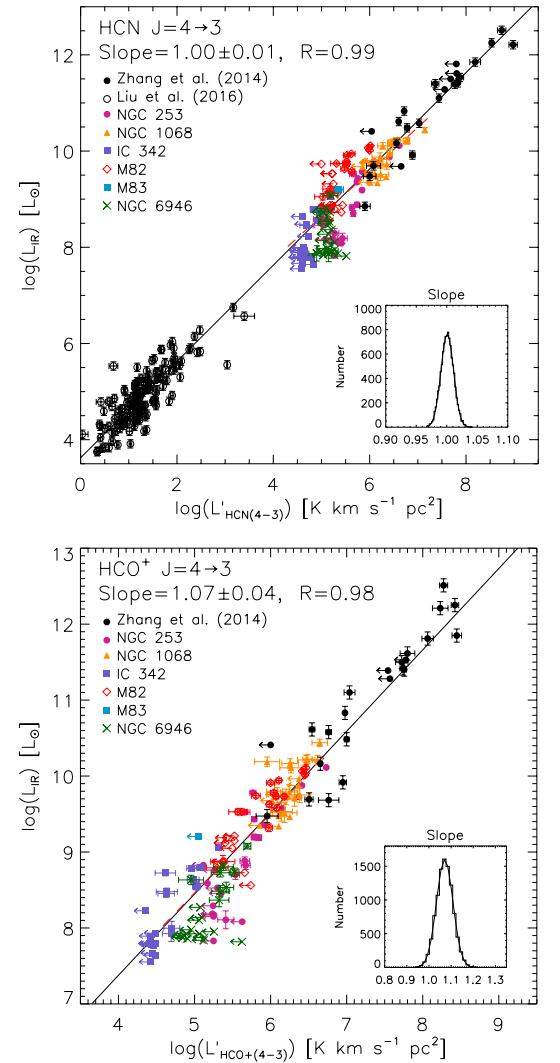
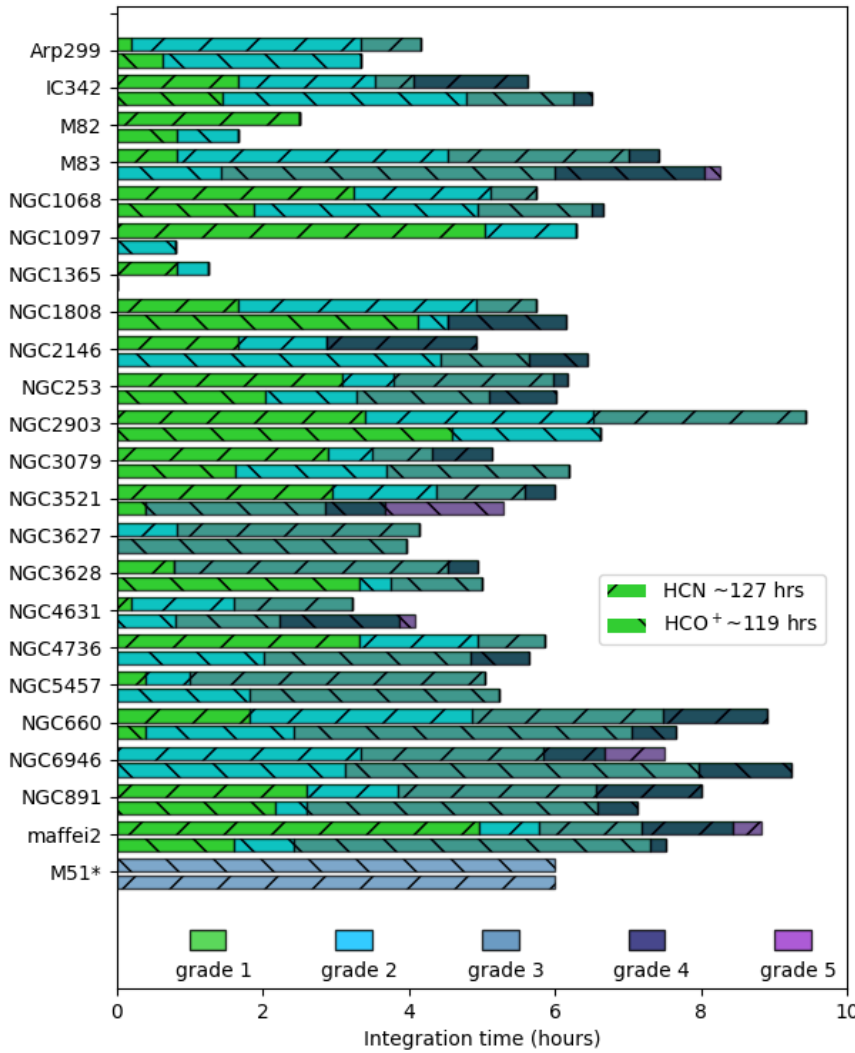


Figure 21: Left: The distributions of the ~ 246 hrs of MALATANG on-source integration time obtained so far as a function of 1) target ID, 2) HCN(4-3) vs. HCO⁺ line, and 3) weather grade. This plot is taken from the MALATANG overview paper (from Zhang et al., in prep.). M 51 is observed as another MALATANG-linked JCMT project (PI: H. Chen, M15BI069 & M16AP052). Right: Early MALATANG science results from Tan et al., in prep. showing the $L'_{\text{HCN}(4-3)} - L_{\text{IR}}$ (top) and $L'_{\text{HCO}+(4-3)} - L_{\text{IR}}$ (bottom) relations based on 6 MALATANG sources (coloured data points) as well as literature data. Already, with only six sources, MALATANG is bridging the luminosity gap between Galactic GMCs (Liu et al. 2016) and integrated galaxies (Zhang et al. 2014). In the case of HCO⁺, MALATANG is probing a new part of the parameter space.

for a statistically significant sample of nearby galaxies makes MALATANG a unique survey. MALATANG is the first such survey carried out on the JCMT – and also one of the largest of its kind on any telescope. MALATANG consists of a total of 91 astronomers (from students to professors) – distributed amongst the EAO member countries as well as the UK and Canada.

What has been happening?

Since MALATANG observations began on Nov. 28th 2015, data have been ‘flowing in’ at a steady pace – largely due to the moderate weather requirements of the survey, as well as extended periods of SCUBA-2 down-time. Thus, at the time of writing about 79% of the total 390hrs of time allocated to MALATANG has been observed, and HCN(4-3) and HCO+(4-3) observations have been carried out for all targets (see Figure 21, left panel).

Our customized version of the Starlink ORAC-DR data-reduction pipeline is now routinely applied to the data as they come

in, producing final, high-quality, data products ready for analysis. In parallel to this, we have developed a new independent data-reduction pipeline based on the GILDAS/CLASS software package. The first internal data release – i.e., shared within the collaboration – of the data products based on the ORAC-DR pipeline has been shared on <http://apps.canfar.net/vosui/#/MALATANG/dr0.1>. Future data releases will include data-cubes reduced with our new GILDAS/CLASS based pipeline.

With a significant portion of the data secured and reduced, the detailed analysis and interpretation of the data has begun in earnest. We find that, in a significant fraction of the sample, the HCN and HCO+ J = 4 - 3 line emission is approximately half as strong as expected. This is an interesting result in and of itself since it suggests very low levels of dense gas excitation in these galaxies. Despite the challenges in detecting HCN and HCO+ J = 4 - 3 in some galaxies, new exciting science results are emerging from MALATANG and are currently in the process

of being written up for publication in peer-reviewed journals. A taste of some of the results is shown in Figure 21 (right panels), which shows the resolved IR - HCN and IR - HCO+ luminosity relations for six of the MALATANG targets (see Tan et al., in prep.). In October 2016 the first face-to-face MALATANG team meeting was held at the Purple Mountain Observatory in Nanjing; this was a highly successful meeting where MALATANG-related science was discussed and where data-reduction teams – as well as the various paper writing ‘tiger teams’ – could discuss and further coordinate their efforts. Also, possible future MALATANG-related proposals on the JCMT and other facilities were discussed. In February 2017 a public MALATANG web site was launched (<http://www.star.ucl.ac.uk/~tgreve/MALATANG>).

In summary, MALATANG is well under way on all fronts – in terms of data acquisition, data reduction, project visibility and publications.

JINGLE: an update

Amelie Saintonge on behalf of the JINGLE team

The JINGLE survey is designed to provide a clear overview of the properties of dust and gas in star-forming galaxies in the Universe today. We are using SCUBA-2 to map the emission from cold dust grains, and the RxA receiver to pick up emission from the carbon monoxide molecule. Combining these observations with data products from Herschel and SDSS surveys, we are quantifying the delicate inter-

play between the physical conditions in the cold interstellar medium and the global properties of galaxies such as their masses, star formation rates, morphologies and environments.

Observations for JINGLE are now 66% complete, and in particular we have made great progress on the SCUBA-2 component of the survey, thanks to excellent weather conditions over-

all on Maunakea these past two winters. Our international team, composed of 102 scientists from 38 institutions across all 6 EAO member and partner regions, has been developing a full suite of data reduction and analysis tools to extract the most information possible from our rich dataset. In particular, we are showing how the specific details of the method used to model the far-infrared spectral

energy distribution of galaxies has a large impact on the dust properties derived, and how quantities such as the dust temperature, mass and grain composition vary across the galaxy population. This has important implications for studies of dust in distant galaxies, where information is more limited and assumptions have to be made.

Our measurements of the molecular gas contents of the JINGLE targets is revealing how well, relatively speaking, we understand how the total amount of cold gas in galaxies depends on their global properties. This allows us to push our investigations further, by making use of the synergy between JINGLE and the SDSS-IV MaNGA survey. The spatial resolution provided by MaNGA makes it possible to link the cold gas contents of galaxies with internal processes such as star formation, dynamics and chemical evolution.

An exciting but somewhat unexpected development for JINGLE has been the detection of background sources around our target galaxies for which

no counterparts can be seen in optical images. Some of these galaxies are not even detected in Herschel images (see image). The most likely explanation for this is that they are very distant dusty galaxies, so distant in fact that the peak of the far-infrared emission has been redshifted into the SCUBA-2 850 μ m band. If confirmed, these galaxies would

be some of the brightest, most distant submillimeter galaxies observed to date. We are now following up to confirm these objects as high redshift galaxies using IRAM and ALMA. By acting as a large area blind survey, JINGLE may provide us with insights about dust in galaxies in both nearby and distant galaxies!

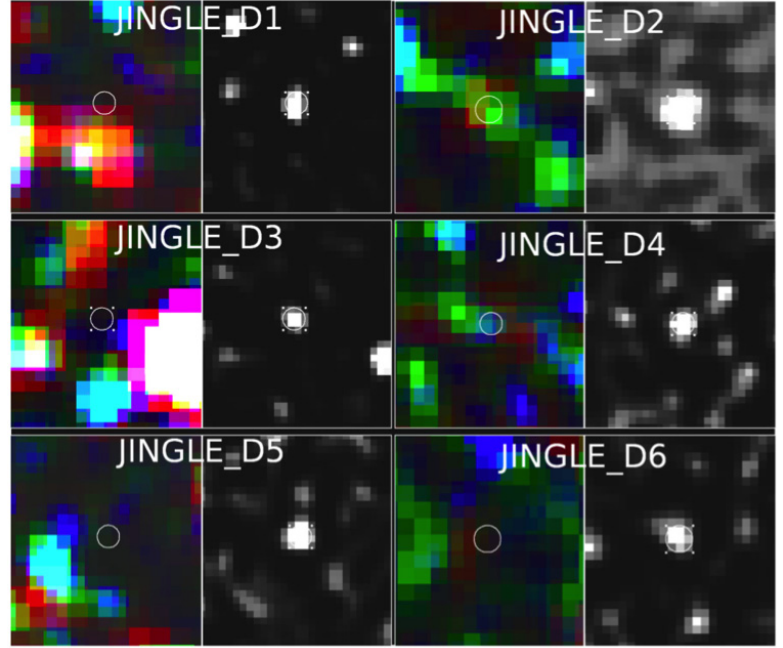


Figure 22: Six possible very distant and dusty galaxies serendipitously detected by JINGLE. Because these objects are not found in Herschel images (left) but are bright in the SCUBA-2 850 μ m images (right), they are candidates for being some of the most distant submillimeter galaxies observed to date.

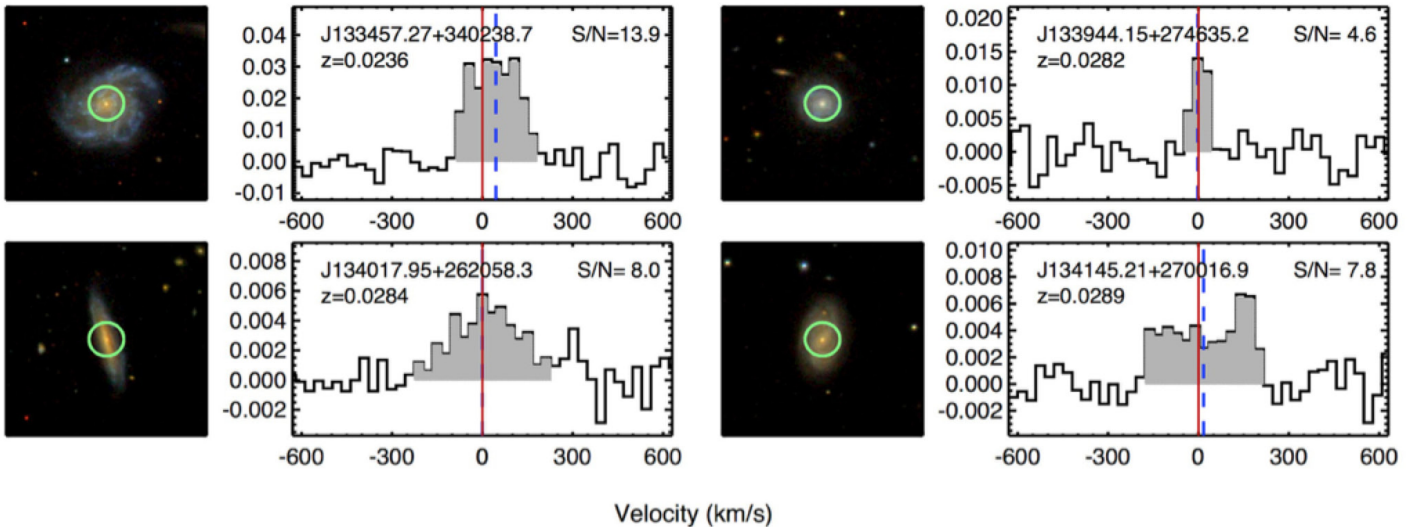


Figure 23: Examples of JINGLE galaxies and their JCMT CO(2-1) emission line detections. The images on the left are from SDSS, with the circle representing the position and beam size of the observations, while the spectra are shown on the right.

S2COSMOS: An EAO Survey of the 2 square degree COSMOS field

James Simpson on behalf of the S2COSMOS team

Over the past eighteen months an EAO consortium has been undertaking an ambitious survey to map the whole COSMOS field with SCUBA-2: S2COSMOS. Selected as a EAO Large Programme, the goal of S2COSMOS is to create the largest, contiguous deep 850 μ m map of the extragalactic sky – of the 2 square degree COSMOS field. COSMOS is the pre-eminent ALMA-visible, degree-scale extragalactic survey field and is the prime location in which to relate the obscured activity traced by observations with SCUBA-2 to the full-range of galaxy populations and environment out to the highest redshifts.

The key feature of S2COSMOS is the combination of both a deep and a panoramic submillimetre map of the complete COSMOS field. Our goal is to obtain a sample of over 1,000 submillimetre sources in this field to a 4- σ flux limit of >4.5mJy (correspond-

ing to a bolometric luminosity of $\sim 5 \times 10^{12} L_{\odot}$). To achieve this our survey builds upon the partial coverage of the COSMOS field provided by the SCUBA-2 Cosmology Legacy Survey (S2CLS; $\sigma_{850} \sim 1.5$ -5mJy, Geach et al. 2017), as well as existing archival data. In this regard S2COSMOS can be considered as the natural extension to the highly successful S2CLS project (Geach et al. 2017), which was undertaken with the JCMT from 2011-2015, and targeted seven key extragalactic survey fields.

Although the COSMOS field was a key target for S2CLS the final map produced from that survey was both relatively shallow and inhomogeneous (Figure 24). The observation strategy for S2COSMOS has thus consisted of two steps: first homogenising the existing SCUBA-2 coverage of the 2 square degree field; before then uniformly increasing the depth of the coverage over the

full 2 square degrees. On June 2nd 2017, observing for S2COSMOS was completed, with all 223hrs of the time allocation used. Data reduction and analysis is being led by survey scientist James Simpson at ASIAA/NAOJ, and the current version of the S2COSMOS map reaches a depth of <1.3mJy across the full 2 square degree COSMOS field (Figure 26).

Using the current S2COSMOS map we have defined a preliminary MAIN sample of 850 μ m sources that are located within the HST/ACS coverage of COSMOS. There are 946 MAIN catalogue sources within the HST/ACS region (defined as having $\sigma_{850} < 1.6$ mJy and >4- σ significance; Figure 26), along with a further 186 supplementary (SUPP) sources that lie outside this footprint but within the Spitzer/IRAC imaging ($\sigma_{850} < 4$ mJy and >4- σ significance). S2COSMOS now represents the largest sample of 850 μ m—selected sources over a

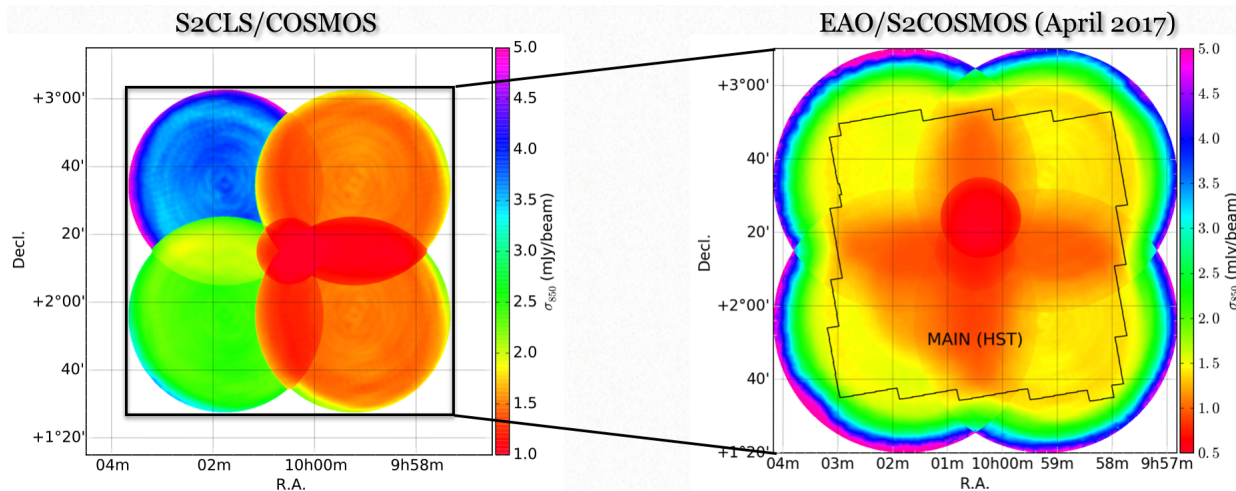


Figure 24: The coverage map of the COSMOS field from the S2CLS survey (Left: 2011-2015) compared to that currently achieved by our ongoing EAO large program S2COSMOS (Right: inc. archival data). These are shown as a noise map to demonstrate the depth achieved across the field. S2COSMOS has made impressive progress at homogenising the earlier S2CLS map and as of April 2017 has reached a depth of <1.3mJy across the full 2 square degree field.

contiguous area. The availability of this uniquely large sample of 850 μ m-selected submillimetre sources in a single field with superb supporting multiwavelength data will provide the opportunity to address a wide range of sci-

ence questions relating to submillimetre galaxies.

The primary science aim of the S2COSMOS survey is to detect a sufficiently large sample of submm sources with which to investigate the spatial clustering of the submm galaxy population. Clustering measurements provide information about the mass of the dark matter haloes in which these sources reside and provide one of the most powerful ways in which to link the submm galaxy population to other galaxy populations at both low- and high-redshift which may represent their potential descendants and progenitors (local ellipticals, QSOs, high- z galaxies etc.). Crucially, for a given sample size, the clustering signal is more easily recovered if the sample is selected

from a contiguous area (compared to an equivalent number of sources selected across different patches of the sky) making COSMOS the ideal field in which to perform a clustering analysis. An initial analysis by members of the S2COSMOS team finds evidence for a strong clustering signal from the sources detected in the S2COSMOS map, with the significance of the detection expected to improve rapidly as the depth of the map is increased further.

The S2COSMOS source catalogue has formed the basis of a number of follow-up studies with ALMA, VLT, Subaru, Keck, and the SMA to determine key properties such as precise positions, redshifts, dynamics, gas masses etc. One highlight of our multi-wavelength follow-up has been SMA observations of a small number of the brightest sources in COSMOS (PI: S. Chapman). The high-resolution imaging with

the SMA directly locates the galaxy responsible for the $850\mu\text{m}$ emission detected by SCUBA-2, facilitating detailed spectroscopic follow-up observations. In Figure 25 we show one such bright S2COSMOS source that is resolved into two individual SMGs, the brightest of which is detected with a flux density of $18.6 \pm 0.7 \text{ mJy}$. Armed with a precise position, follow-up spectroscopy with the LRIS instrument on Keck-1 demonstrates that this bright SMG lies at a redshift of $z=2.5$, making it one of the most intrinsically luminous starbursts known to date and the brightest in the entire S2CLS and S2COSMOS catalogue. As such it pushes the extremes of sustainable star formation in a single galaxy, and will be a remarkable laboratory for studying star formation at high redshift. At the same time, the neighbouring 3 mJy source shows that multiplicity is still a factor in identifying very bright sources, and the sum of

the components is in excellent agreement with the SCUBA2 detection.

Already the S2COSMOS project has already detected well over 1,000 robust submm sources, over an area twice the size of comparable surveys. The S2COSMOS team (comprised of 111 researchers across all EAO partner regions) is using this map to make unique tests of the clustering of the submm galaxy population on scales up to

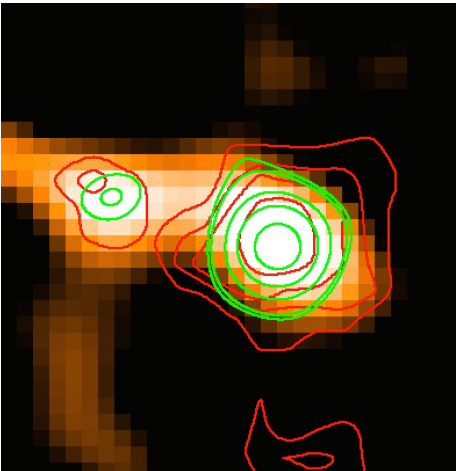


Figure 25: IRAC $4.5\mu\text{m}$ image of a bright SMG identified in the S2COSMOS survey. Overlaid are contours representing emission traced by the SMA (green) and VLA (red). The SMA observations resolve the SCUBA-2 detected source into two submm galaxies, the brightest of which is detected at a flux density of $18.6 \pm 0.7 \text{ mJy}$. Follow-up spectroscopy with LRIS/Keck demonstrates that this bright SMG lies at a redshift of $z=2.5$ and confirms it as one of the most luminous (non-lensed) starbursts identified to date, and the brightest across the S2CLS and S2COSMOS observations.

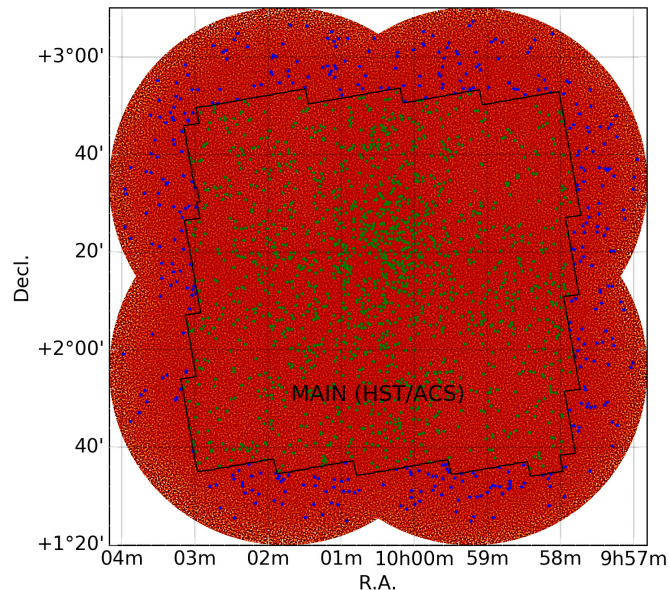


Figure 26: The S2COSMOS image of the COSMOS field at $850\mu\text{m}$. We identify 946 sources (green) at a $\text{SNR} > 4\sigma$ that lie within the HST/ACS coverage (MAIN sample) and a further 186 sources at a $\text{SNR} > 4\sigma$ that lie outside this uniform coverage region (SUPP; $\sigma_{850} < 4 \text{ mJy}$). We predict that when completed our survey will yield a sample of > 1500 submillimetre sources across the full COSMOS field.

~60 Mpc, study evolution in the properties of starburst galaxies with redshift, and conducting sensitive stacking analyses that will unveil the far—infrared prop-

erties of a huge range of galaxy populations in this very well studied field.

S2COSMOS Survey Scientist:

James Simpson (ASIAA/NAOJ). Coordinators: Scott Chapman (CA), Yuichi Matsuda (JP), Ian Smail (UK), Ran Wang (CN), Wei-Hao Wang (TW), Yujin Yang (KR).

STUDIES - The SCUBA-2 Ultra Deep Imaging EAO Survey

Wei-Hao Wang on behalf of the STUDIES team

STUDIES is a SCUBA-2 450 μ m program imaging the COSMOS/CANDELS region. With 330 hours of observing time awarded, the goal is to reach the confusion limit (rms < 0.6 mJy) for the first time at this waveband, and to go more than 10x deeper than Herschel at 250-500 μ m. We made good progress in the 2015/2016 winter and accumulated 165 hours of observations. A noise of ~0.8 mJy is reached in the map center. Unfortunately, no more data have been col-

lected since then, because of instrumental problems and poor weather. However, we carry on with the scientific analyses of the data taken thus far and had submitted the first science paper from this project.

In Simpson et al. (2017), we studied ZF 20115, a $z = 3.717$ galaxy that was claimed to be a “post-starburst” passive galaxy by Glazebrook et al. (2017) because of its strong Balmer break and absorption lines. Glazebrook

et al. also inferred an unusually early formation epoch that may challenge the current model of galaxy formation. However, we found it detected in deep ALMA 870 μ m and our SCUBA-2 450 μ m images (Fig.1). The ALMA detection (1.4 ± 0.2 mJy) is about 0.4 arcsec offset from ZF 20115, typical among high-redshift submillimeter galaxies. STUDIES also detects this galaxy at 450 μ m (3.1 ± 1.0 mJy). The STUDIES 850 μ m flux (1.49 ± 0.15 mJy) is consistent with the ALMA value, although this flux is generally considered as below the confusion limit at 850 μ m. The 450 μ m and 850 μ m detections imply a dusty starburst at $z = 3.717$ with an infrared luminosity of $\sim 7.7 \times 10^{11} L_{\odot}$ and a star formation rate of $\sim 100 M_{\odot}/\text{yr}$. This is nearly an order of magnitude fainter than the detection limit of Herschel at $> 100 \mu\text{m}$, and this is why this galaxy was previously considered as “passive.” After taking into account the obscured star-forming component in this system, we found a 50% lower stellar mass. This removes the need for a very high formation redshift and thus removes the tension with models. This study clearly demonstrates the reason for our deep 450 μ m imaging: the majority of high-redshift dusty star-forming galaxies are fainter than the Herschel confusion limits.

We also use STUDIES data taken

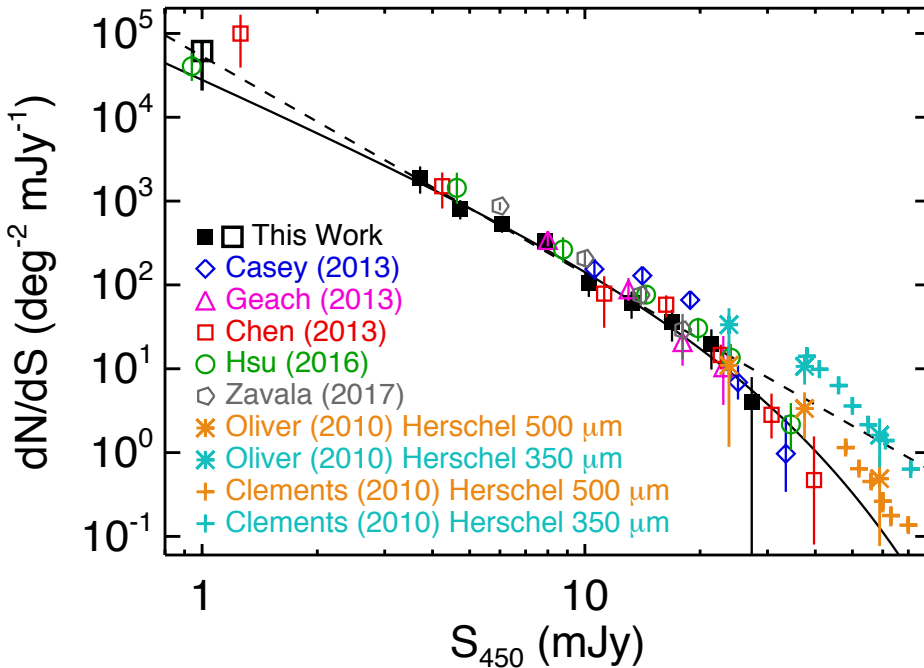


Figure 27: 450 μ m counts. Black filled squares are counts derived from 4σ sources in STUDIES. They are deeper than all other blank-field counts in the literature. The solid curve is a Schechter fit to the black filled squares, and the dashed line is a power-law fit without using the brightest flux bin. The black open square is derived with a $P(D)$ analysis. It is consistent with the power-law extrapolation from the bright end, and also consistent with counts derived from the two lensing cluster surveys at ~ 1 mJy.

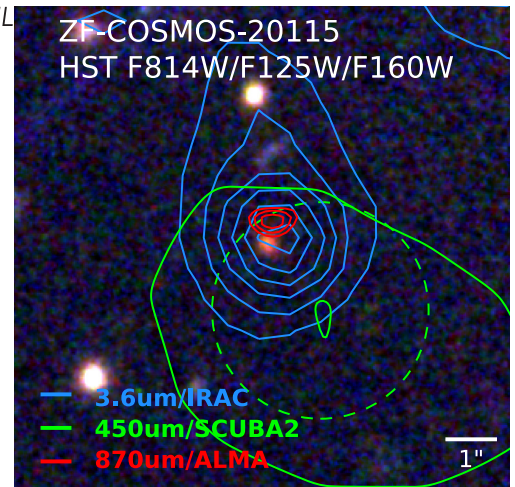
in 2015/2016 to derive the $450\mu\text{m}$ counts (Fig.2). We have reached deeper than all previous $450\mu\text{m}$ blank-field surveys. Our counts show a perfect power law at 1–20 mJy, and are consistent with previous studies. We plan to submit this paper in May or June 2017.

Reference

Glazebrook, K., et al. 2017, *Nature*, 544, 71

Simpson, J. M., et al. 2017, *ApJL*, submitted, arXiv:1704.03868

Figure 28: ZF 20115, the red galaxy at the center of the HST 0.8–1.6 μm color image. The red contours show the ALMA 870 μm detection and the green contours show our STUDIES 450 μm detection. The 450 μm positional uncertainty is shown with a dashed circle.



The JCMT Ohana - aloha and a hui hou

Harriet Parsons, Craig Walther, JCMT

The EAO/JCMT ohana (*family*) here in Hawaii is a wonderfully diverse group of astronomers, telescope operators, engineers, software programmers, administration and finance specialists, working hard to produce the best science. It is sad to say that this year we say a *hui hou* "Until we meet again" to three of our staff members.

On 31st August, Iain Coulson retired from his position as JCMT Senior Support Scientist. Iain joined the JCMT staff in 1986, at a time when the telescope was still being commissioned, in a

position advertised as being a Telescope Operator cum Support Scientist cum Researcher. The post evolved over time in roughly that order, with operations foremost in the early days; Iain was the JCMT Operator during the first half of the 1991 Total Solar Eclipse. Visiting observers started arriving in Semester M (what would be 1987B in today's money); they needed support then, and they need it now (and by all accounts appreciate what they get), and Iain has been a stalwart member of the support team throughout.

He is perhaps best known for developing and maintaining the pointing model of the telescope, including the generation of the refraction model, and the incorporation of a model of the antenna track profile derived by 'inclinometry'. He was the UK Queue Manager and Technical Secretary to the UK Time Allocation Committee for many years, became Telescope Scheduler and Tech.Sec to the ITAC for the later years of operations under the Joint Astronomy Centre, and was Tech.Sec to the TAC in the first years of the EAO. Iain's research has included the SCUBA



Figure 29: The EAO/JCMT staff say a fond farewell to (left to right) Iain Coulson, Malcolm Currie and E'Lisa Lee.

mapping of debris disks around Vega, Fomalhaut and Eps Eridani, and, for the last decade or so, he has played the leading observational role in a campaign to assess the physical and chemical properties of cometary comae.

Malcolm Currie retired from Rutherford Appleton Laboratory (RAL) in April. Malcolm was a longtime participant in the Starlink project. He was the principal developer of the KAPPA software, and he was Starlink's leading expert on FITS. Malcolm made two extended stays in Hawaii where he was a principal developer of the ORAC-DR system and later managed the Scientific Computing Group for several years. He was heavily involved in improvements to the heterodyne ORAC-DR pipeline, and actively participated in many different observing programs including, most recently, the GBS and COHRS. The last two years Malcolm has supported the Starlink community and users of JCMT and UKIRT data out of RAL. Malcolm's expertise in ORAC-DR, infra-red data processing and heterodyne data processing will be greatly missed.

E'Lisa Lee is leaving us this year as she continues her interest in astronomy at graduate school. E'Lisa has been working as a telescope operator for EAO during extended observing for the past two years. In addition to her duties as an extended operator, E'Lisa has been responsible for checking nightly data quality, publication statistics and recently undertook a small research project linked to the Transient Program.

As sad as it is to see these brilliant staff members leave we are thrilled to welcome and say *aloha* to some new and not-so-new faces. John Kuroda comes back to the JCMT after working for ASIAA on the YTLA, SMA, and GLT. He used to work for the JCMT under the JAC organisation and is now back working at JCMT as computer programmer. In addition John is also working towards both a B.A. in Mathematics and a B.S. in Computer Science.

With the departure of Iain Coulson we are excited to announce the new hire of Support Astronomer Steve Mairs. Steve is a familiar name amongst JCMT SCUBA-2 users. He recently handed in his thesis at the University of

Victoria in Canada, where he was supervised by Doug Johnstone. His thesis focuses on large scale and small scale structures in the Gould Belt star forming regions, and variability protostars in the submillimeter. If you recognise his name it may be that you read his paper "The JCMT Gould Belt Survey: a quantitative comparison between SCUBA-2 data reduction methods" Mairs et al. 2015. Steve is looking forward to setting in to island life with his wife Desiree.

Skye is perhaps the youngest new member of the JCMT ohana in Hawaii. JCMT telescope operator Callie Matulonis gave birth to Skye in September. Staff have been thrilled when Callie brings little Skye to the office.

Along the same lines, last year Xue-Xiang, an active lead member of the MALATANG program celebrated the birth of his son Xin-Tong Jiang.

Most recent of all the JCMT staff are delighted to be able to send their congratulations to Ciska Kemper, frequent JCMT user and former TAC chair, who gave birth to a little girl, Irene, in May.



Figure 30: Left to right: Ciska and Irene (born May 2017), Skye Wala Matulonis (born September 2016) Xin-Tong Jiang (born May 2016, son of Xue-Jian Jiang). John Kuroda returns to the JCMT office in Hilo, new support scientist Steve Mairs.

